

Two-Tier Multi-Rate Slotted ALOHA for OWC/RF-Based IoT Networks

Milica Petkovic, *Member, IEEE*, Dejan Vukobratovic, *Senior Member, IEEE*,
Andrea Munari, *Member, IEEE*, and Federico Clazzer, *Member, IEEE*

Abstract—We consider a massive Internet of Things (IoT) scenario where indoor IoT devices access the network via optical wireless communication (OWC) IoT systems that relay data via a backhaul radio frequency (RF) low-power wide-area network (LP WAN). We propose a novel two-tier multi-rate Slotted ALOHA (SA) system model to design and analyse such hybrid OWC/RF networks. For a particular hybrid OWC/RF setup, we present an in-depth numerical investigation that provides insights into the proposed two-tier multi-rate hybrid OWC/RF SA system design.

Index Terms—Internet of Things (IoT), Optical Wireless Communications (OWC), Slotted ALOHA (SA).

I. INTRODUCTION

BEYOND 5G networks aim to provide energy and spectrally efficient massive IoT connectivity for extreme connection densities [1]. The main challenge lies in providing wide-area coverage for sporadic and unpredictable transmission of short packets from a vast number of devices [2]. Low-power wide area networks (LP WAN) such as LoRa and NB-IoT are recent massive IoT solutions operating in sub-GHz radio frequency (RF) bands [3]. Due to short packets and unpredictable device activity, their system design relies on cost-effective random access (RA) protocols, such as the variants of Slotted ALOHA (SA) [4]–[6].

To relieve pressure from conventional RF-based LP WANs, optical wireless communications (OWC) have been recently considered as an emerging complementary technology. For indoor environment, OWC technology operating in visible or infrared (IR) spectrum is a suitable license-free short-range connectivity solution [7]. OWC IoT relies on low-cost OWC transceivers to provide low-rate indoor IoT connectivity, either in a stand-alone or a hybrid OWC/RF setup. Indoor OWC IoT based on the SA policy has been recently analyzed in [8]–[14].

In this paper, we propose and analyse a hybrid OWC/RF massive IoT network based on a novel *two-tier multi-rate* SA system design. The first tier comprises a collection of isolated indoor OWC IoT networks connected to a network infrastructure via the second-tier outdoor RF-based LP WAN. OWC IoT devices contend for access using SA in their respective indoor OWC cells and, if successful, their packets are relayed to the second tier where they contend for SA-based

access via the outdoor LP WAN (Fig. 1). The SA protocol at the LP WAN tier operates at M times higher slot rate relative to the OWC tier, where judicious adaptive selection of factor M based on the operating parameters of the hybrid OWC/RF IoT system is crucial for optimized system performance.

The contribution of the paper is summarized as follows:

- 1) We consider a novel architecture for future massive IoT which combines short-range OWC and LP WAN technologies. The motivation is to reduce the connection density of RF-based LP WANs by offloading indoor devices to the OWC-based IoT.
- 2) The proposed architecture is based on two-tier SA protocols, previously considered in the context of sensors networks [15]. Due to OWC-RF data rate difference, we expand this model into two-tier *multi-rate* SA applicable across the number of emerging use cases (e.g., drones or low-Earth orbit satellites that connect remote IoT devices to the network).
- 3) We present detailed analysis of packet error/outage rates at both OWC and LP WAN tiers. Combining these results into the overall system throughput, we use numerical results to provide guidelines for the system design. We emphasize the benefit of the *multi-rate* SA design, where adaptive control of the slot rate factor M notably improves the system throughput. We consider the optimal indoor OWC cell design by exploring the effects of OWC cell parameters on the system performance.
- 4) For the proposed two-tier multi-rate SA system, we consider concrete OWC and RF models. Specifically, we assume SA with capture and multi-packet reception (MPR) for indoor OWC tier, and LoRa-inspired model proposed in [16] for outdoor LP WAN tier. Note that the model is sufficiently general to include other specific models at both tiers.

In our previous work [12], we focused on the design of single indoor OWC IoT cell. In a parallel work [13], we considered two-tier OWC/RF massive IoT setup and analysed its fundamental behaviour using the tools from stochastic geometry, while in [14] two-tier OWC/RF system is proposed considering a single large indoor OWC IoT system with a large number of indoor OWC access points (APs). In contrast, this work explores a novel two-tier *multi-rate* SA design and develops a detailed system analysis and design for specific design assumptions at both OWC and RF tiers.

II. TWO-TIER MULTI-RATE SLOTTED ALOHA

We consider a set of K indoor OWC IoT systems deployed across a wide area to connect indoor OWC IoT devices to their respective OWC APs within, e.g., a smart home environment. Each system contains U IoT devices that access the OWC

M. Petkovic and D. Vukobratovic are with University of Novi Sad, Faculty of Technical Science, 21000 Novi Sad, Serbia (e-mails: milica.petkovic@uns.ac.rs; dejanv@uns.ac.rs).

A. Munari and F. Clazzer are with Institute of Communications and Navigation of the German Aerospace Center (DLR), 82234 Wessling, Germany (e-mails: andrea.munari@dlr.de; federico.clazzer@dlr.de).

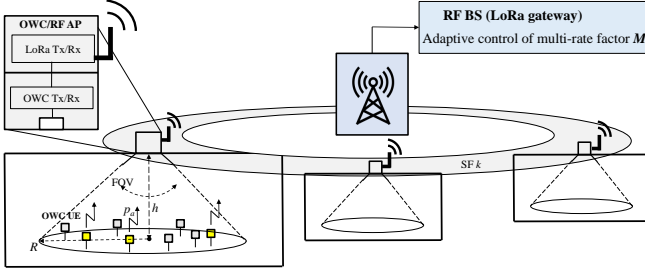


Fig. 1. Two-Tier OWC/RF-Based IoT Network.

AP using SA protocol. Each IoT device transmits a fixed-length data packet during a slot of duration T_{owc} . During each slot, the OWC AP attempts to decode data packets from the received signal. We consider a receiver model for OWC AP where multiple packets originating at multiple active devices are decoded by exploiting the capture effect. The OWC APs operate as decode and forward (DF) relays, where the packets decoded during a single OWC slot are transmitted during the following RF slots as described below.

The K indoor OWC IoT APs are connected to the BS via a LP WAN RF-based network. To be more specific, we assume the outdoor LP WAN is based on LoRa physical layer and uses SA multiple access with slot duration $T_{\text{rf}} \leq T_{\text{owc}}$ ¹ LoRa PHY is based on a Chirp Spread Spectrum modulation scheme [16], improving robustness against interference and multipath fading. Besides, it uses quasi-orthogonal spreading factors (SFs), meaning that the users with different SFs will cause negligible inter-SF interference to each other [16], [17]. If LoRa users are closer to the BS, transmission at lower SF will be adopted leading to the lower reception sensitivity, decreased processing gain, as well as shorter chirp symbol length and higher data rates (see Sec. II.2). Hence, based on distance d_{SF} between OWC IoT APs and the BS, the BS is in charge to assign $\text{SF} \in \{7, 8, \dots, 12\}$ while maintaining constant bandwidth (BW). This affects the chirp symbol duration as $T_s = 2^{\text{SF}}/\text{BW}$, as well as data rate and slot duration T_{rf} [16].

Since we assume negligible inter-SF interference, we will focus on a set of indoor OWC APs that use the same SF while transmitting to the LP WAN BS. This means that all K indoor OWC APs are located at the approximate distance d_{SF} from the gateway (more precisely, being inside the ring of the radius $d_{\text{SF}} \pm 1$ km), as it is depicted in Fig. 1. Additionally, we assume that the OWC slot duration T_{owc} is dependent on the slot duration T_{rf} at the LP WAN as $T_{\text{owc}} = M \cdot T_{\text{rf}}$ ($M \in \mathbb{N}/0$). For a given BW, the value of SF will determine the chirp symbol length T_s , and consequently the RF slot duration T_{rf} , and data rate of RF transmission. By adjustment and adaptive control of multi-rate factor M , the LoRa BS effectively controls the slot rate as $T_{\text{owc}} = M \cdot T_{\text{rf}}$ in the OWC sub-systems, as well as a data rate of OWC transmissions. In this way, the LoRa network is capable to keep a constant BW while providing adaptive data rates determined by M in our overall system

¹Slot synchronisation incurs slightly increased system complexity as compared to commonly used LoRaWAN which uses spread-ALOHA.

model. For simplicity, we assume the indoor OWC systems are slot-synchronized, and the outdoor RF system slot is aligned with M consecutive OWC system slots. Clearly, the RF system operates at M times higher data rate.

1) *Indoor OWC IoT Network:* We consider the SA scheme with Bernoulli arrivals to model the distribution of the number of active users in a given slot for all indoor OWC systems. This means that each of U IoT devices becomes activated in a given slot with probability p_a independently of any other user. Assuming that $U_a^{(i)}$ represents the number of activated users in the i -th OWC IoT system in a given slot ($i = 1, \dots, K$), it holds $\mathbb{P}[U_a^{(i)} = u] = \binom{U}{u} p_a^u (1 - p_a)^{U-u}$ with $U_a^{(i)}$ being a binomial random variable with mean $U p_a$.

The IoT devices employ LED-based transmitters operating in the IR spectrum and employing intensity modulation with on-off keying to satisfy non-negative constraint. All OWC APs include photodetectors as OWC receivers based on direct detection of the light intensity. In each of the K indoor OWC systems only the line-of-sight (LoS) component of the optical signal is considered since the reflected signals energy is significantly lower [7]. A Lambertian channel model for the LOS link is adopted², as well as the assumption that U IoT devices are uniformly placed on a horizontal plane³ within the circle of radius R . The SNR of the OWC link between the j -th user and the i -th OWC AP is defined as $\gamma_{\text{owc}}^{i,j} = P_t^2 h_{i,j}^2 \eta^2 / \sigma_n^2$ ($i = 1, \dots, K, j = 1, \dots, U_a^{(i)}$)⁴, where P_t is the transmitted optical power, η is the optical-to-electrical conversion efficiency, while the Gaussian noise variance is determined as $\sigma_n^2 = N_0 B$ with N_0 and B being the noise spectral density and the system bandwidth, respectively. After utilization of the random variables transformation techniques, the probability distribution function (PDF) of signal-to-noise ratio (SNR) γ_{owc} is derived as [12], [13]

$$f_{\gamma_{\text{owc}}}(\gamma) = \frac{(\mu_{\text{owc}} \mathcal{X}^2)^{\frac{1}{m+3}}}{R^2 (m+3)} \gamma^{-\frac{m+4}{m+3}}, \quad \gamma_{\min} \leq \gamma \leq \gamma_{\max}, \quad (1)$$

where L is the distance between horizontal plane where users are located and the ceiling, $\mathcal{X} = \frac{A(m+1)\mathcal{R}}{2\pi} T_g g(\psi) L^{m+1}$, $\gamma_{\min} = \frac{\mu_{\text{owc}} \mathcal{X}^2}{(R^2 + L^2)^{m+3}}$, $\gamma_{\max} = \frac{\mu_{\text{owc}} \mathcal{X}^2}{L^{2(m+3)}}$ and $\mu_{\text{owc}} = P_t^2 \eta^2 / \sigma_n^2$.

²Based on the Lambertian law for modeling the optical LoS link, the intensity of the optical signal between the j -th IoT device and the i -th OWC AP ($i = 1, \dots, K, j = 1, \dots, U_a^{(i)}$) is defined as

$$h_{i,j} = \begin{cases} \frac{A(m+1)\mathcal{R} T_g g(\psi_{i,j})}{2\pi d_{i,j}^2} \cos^m(\theta_{i,j}) \cos(\psi_{i,j}), & 0 \leq \psi_{i,j} \leq \Psi \\ 0, & \text{otherwise} \end{cases}$$

where Ψ is the field of view (FOV) of the receiver, A is the physical area of the detector, \mathcal{R} is the responsivity, T_g denotes the gain of the optical filter, while $g(\psi_{i,j}) = l^2 / \sin^2(\Psi)$, for $0 \leq \psi_{i,j} \leq \Psi$, is the the optical concentrator with l being the refractive index of lens at a photodetector. The Lambertian order of the light source is $m = -\ln 2 / \ln(\cos \Phi_{1/2})$, where $\Phi_{1/2}$ represents the semi-angle at half power of LED. Distance, irradiance angle and incidence angle between the j -th IoT user and the i -th OWC AP are defined by $d_{i,j}$, $\theta_{i,j}$ and $\psi_{i,j}$, respectively.

³For uniform distribution of the IoT users placed on horizontal plane within the circle of radius R , the PDF of the radial distance r of a randomly placed user from an OWC AP receiver is $f_r(r) = 2r/R^2$, $0 \leq r \leq R$.

⁴In the following, we omitted the indexes i and j for better clarity.

The cumulative distribution function (CDF) of the SNR is [13]

$$F_{\gamma_{\text{owc}}}(\gamma) = \begin{cases} 1 + \frac{L^2}{R^2} - \frac{1}{R^2} \left(\frac{\mu_{\text{owc}} \mathcal{X}^2}{\gamma} \right)^{\frac{1}{m+3}}, & \gamma_{\min} \leq \gamma \leq \gamma_{\max} \\ 1, & \gamma > \gamma_{\max} \end{cases} \quad (2)$$

SA with Capture and MPR: Regarding the OWC tier, SA with capture with MPR is considered. For SA with capture, a packet can be decoded only if the received SNR over OWC link, γ_{owc} is above a previously determined threshold, denoted by γ_{th} . The probability that packet will not be decoded can be determined by the CDF defined in (2) as

$$P_{\text{er}} = \mathbb{P}[\gamma_{\text{owc}} < \gamma_{\text{th}}] = F_{\gamma_{\text{owc}}}(\gamma_{\text{th}}). \quad (3)$$

This kind of SA with capture within OWC can be easily implemented by exploiting different spread spectrum techniques with the aim to reduce the impact of the interference and to improve security of transmission [18].

Additionally, MPR is also considered as multiple packets from multiple active devices in the same OWC IoT system can be decoded by corresponding OWC AP. We set the maximal number of packet to be possibly decoded to be equal to M - the ratio between slot durations in OWC and RF tiers, determining the maximal load of the LP WAN RF network.

2) *Outdoor Wide-Area RF IoT Network:* If the received power of the packet is among M highest of all received packets at corresponding OWC AP, and the capture condition is satisfied, the packet will be correctly received and randomly assigned to one of M newly formed slots. Also, only one packet can be assigned to each of the new slots. All OWC AP, acting as DF relays, re-encode and forward data packets to the LoRa BS during assigned new slot. RF tier also employs SA approach with different slot duration T_{rf} as defined earlier.

The number of active devices in LoRa system is now determined by the OWC IoT systems and the value of M . While keeping a constant BW, the gateway adjusts the SF based on the distance d_{SF} . As it is presented in Table I, the SF has impact on a bit-rate (for BW=125 kHz), as well as the time-on-air of a transmission and receiver sensitivity (determined by the SF specific threshold q_{SF}). As it was mentioned earlier, for a given value of BW=125 kHz, adjustment of SF will affect the RF slot duration T_{rf} and data rate of RF transmission. Furthermore, a LoRa BS is able to perform adaptive control of parameter M , which directly results in the design of the slot rate T_{owc} in the OWC sub-systems as $T_{\text{owc}} = M \cdot T_{\text{rf}}$, and consequently on a data rate of OWC transmissions.

If a packet from OWC IoT system is successfully decoded, it is forwarded to final gateway with transmit power P_{rf} over Rayleigh distributed block flat-fading channel. The instantaneous SNR of a single end-device can be defined as $\gamma_{\text{rf}} = P_{\text{rf}} g_{\text{SF}} h_{\text{rf}}^2 / \sigma_{\text{rf}}^2$, where h_{rf} is the fading amplitude of the RF link modeled by Rayleigh distribution, $g_{\text{SF}} = (\lambda / 4\pi d_{\text{SF}})^n$ is path loss attenuation function determined by the Friis transmission equation, where λ is the carrier wavelength, n is the path loss exponent to be equal to 2.7 and 4 in urban and sub-urban environments, respectively, and the range d_{SF} is determined by SF in Table I. Additive white Gaussian noise variance σ_{rf}^2 is determined as $\sigma_{\text{rf}}^2 = -174 + \text{NF} + 10\log\text{BW dBm}$, where NF is the receiver noise figure [16].

TABLE I
LoRa characteristics [16]

SF	Bit-rate	T_{rf}	q_{SF}	d_{SF}
7	5.47 kb/s	36.6 ms	-6 dBm	1 km (± 1) km
8	3.13kb/s	64 ms	-9 dBm	3 km (± 1) km
9	1.76 kb/s	113 ms	-12 dBm	5 km (± 1) km
10	0.98 kb/s	204 ms	-15 dBm	7 km (± 1) km
11	0.54kb/s	372 ms	-17.5 dBm	9 km (± 1) km
12	0.29kb/s	682 ms	-20 dBm	11 km (± 1) km

At the BS, a desired packet will be successfully decoded if outage does not happen. In order to determine the outage probability of an uplink transmission, we adopt the model that assumes the outage will happen at the BS if either of following two conditions are satisfied [16]:

Condition I: The instantaneous SNR of the received packet is below the SF specific threshold q_{SF} given in Table I, i.e.,

$$P_{\text{out}}^{\text{I}} = \mathbb{P}[\gamma_{\text{rf}} < q_{\text{SF}}] = \mathbb{P}\left[\frac{P_{\text{rf}} g_{\text{SF}} h_{\text{rf}}^2}{\sigma_{\text{rf}}^2} < q_{\text{SF}}\right]. \quad (4)$$

Since Rayleigh distributed block flat-fading channel is assumed for second tier, h_{rf}^2 represents the channel gain modelled by exponential distribution with mean one. The first outage condition can be determined as

$$P_{\text{out}}^{\text{I}} = \mathbb{P}\left[h_{\text{rf}}^2 < \frac{\sigma_{\text{rf}}^2 q_{\text{SF}}}{P_{\text{rf}} g_{\text{SF}}}\right] = 1 - \exp\left(-\frac{\sigma_{\text{rf}}^2 q_{\text{SF}}}{P_{\text{rf}} g_{\text{SF}}}\right). \quad (5)$$

Condition II: Assuming that the desired signal is the strongest one, by this condition, it should be at least ϵ times stronger than any other signal with the same SF:

$$P_{\text{out}}^{\text{II}} = \mathbb{P}\left[\frac{\gamma_{\text{rf}}}{\gamma_{\text{rf}}^*} \leq \epsilon\right], \quad (6)$$

where γ_{rf}^* represents the instantaneous SNR of interfering signal transmission of the same SF. We adopt $\epsilon = 4$, i.e., Condition II assumes that the desired signal is at least 4 times (6 dB) stronger than any other signal with the same SF.

A graphical example of proposed system transmission is presented in Fig. 2, assuming $K = 5$ OWC IoT sub-systems each containing $U = 5$ users, and multi-rate factor $M = 3$. Depending on the value of p_a , during the n -th slot, a subset of users in each OWC system will be active. In our example, in the first OWC system, Users 1, 2 and 4 will generate the data, in the second OWC system, User 2 will be active, and so on (see Fig. 2). Packets 2.1, 1.3, 3.3, 3.4 and 4.5 will be erased at the OWC AP since their SNRs are assumed lower than γ_{th} due to the SA scheme with capture. Up to M packets can be decoded at each OWC AP, which are randomly assigned to M slots at the LP WAN tier. When number of decoded packets exceeds $M = 3$ (e.g., the 5-th OWC system in our example), packets with higher received power have priority to be forwarded (packet 2.5 will be erased due to the lowest SNR). During the $(n+1)$ -th OWC slot, the second tier uses M RF slots to forward the packets decoded by each of K OWC APs during the previous n -th OWC slot. After LP WAN transmission, some of the packets will be erased in all mini-slots due to Condition I and Condition II. For example, in Fig. 2, packets 4.2, 4.1, and so on are erased, while packets 3.5 and 1.1 will be the only to be decoded.

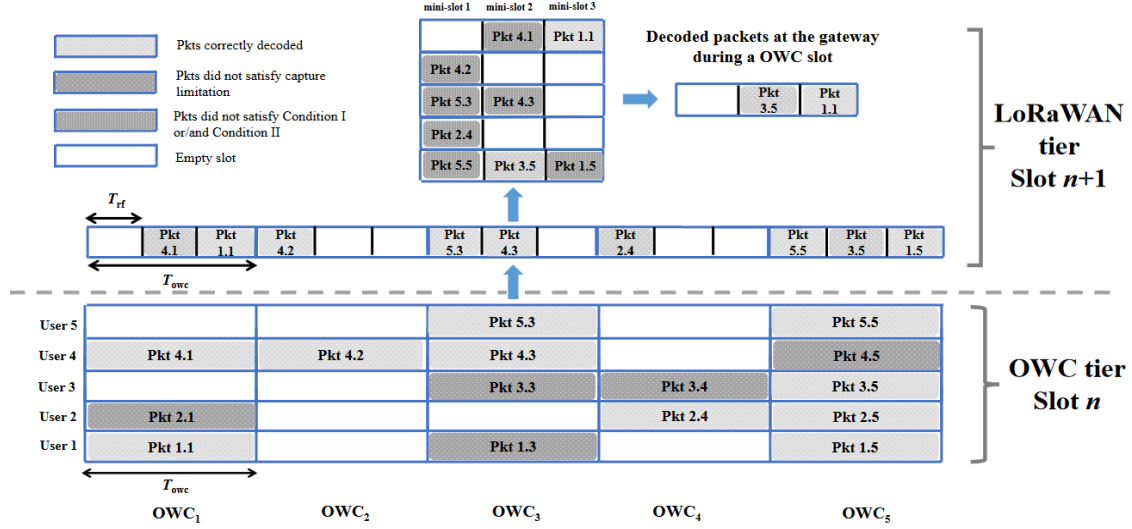


Fig. 2. Example of packet transmission in a OWC slot.

III. NUMERICAL RESULTS AND DISCUSSION

In this section, we present numerical results obtained by Monte Carlo (MC) simulations. We consider throughput depending on activation probability p_a of users in indoor OWC clusters. Note that the throughput is defined by averaging the number of decoded packets per RF slot. For this reason, the maximum throughput will not depend on M . We note that the throughput will linearly increase with M if it is defined as an average number of decoded packets per OWC slot.

Simulation setup: Following values for the parameters are adopted: $\text{FOV} = 90^\circ$, $A = 1 \text{ cm}^2$, $\mathcal{R} = 0.4 \text{ A/W}$, $T_g = 1$, $l = 1.5$, $\eta = 0.8$, $N_0 = 10^{-21} \text{ W/Hz}$ and $B = 200 \text{ kHz}$. Further, $\gamma_{\text{th}} = 0 \text{ dB}$, $P_t = 10 \text{ dBm}$, $\text{NF} = 6 \text{ dB}$, $\text{BW} = 125 \text{ kHz}$, $n = 2.7$, while $P_{\text{rf}} = 14 \text{ dBm}$ as maximal transmit power in Europe, and $\lambda = c/f_c$ when $f_c = 868.1 \text{ MHz}$.

Numerical results: Fig. 3 presents throughput versus p_a for different multi-rate parameter M when the OWC IoT systems are very close to the gateway ($\text{SF} = 7$) and when their distance is larger ($\text{SF} = 11$). Recall that the distance d_{SF} determines both the spreading factor SF and the slot duration T_{rf} (Table I), while the multi-rate factor M determines the slot duration T_{owc} . In general, the values of SF and M directly affect data rates of both tiers. From Fig. 3 we can conclude that maximal throughput occurs for certain optimal value of p_a , which depends on both SF and parameter M . Additionally, for larger p_a , which corresponds to increased number of active users in all OWC IoT systems, higher M results in higher system throughput. As detailed later in the section, by providing adaptive data rates controlled by M , significant improvement of the system performance can be achieved with respect to the LoRa RF range and distances d_{SF} .

Further, in Figs. 4 and 5 we observe how indoor OWC parameters affect the OWC/RF system performance for different data rates at the tiers determined by the parameter M .

Impact of the semi-angle $\Phi_{1/2}$ on the overall throughput is presented in Fig. 4 for different M . The value of $\Phi_{1/2}$ determines how the light intensity is distributed over the

receiving plane. When $\Phi_{1/2}$ is larger, LEDs output beam will be wider, thus the received power at the AP will be greater. In that case, the OWC IoT users far distant from OWC AP are likely to satisfy capture condition. With lowering $\Phi_{1/2}$, the OWC users will radiate narrower optical beams, and distant OWC users will not satisfy capture condition. For that reason, when number of active users (i.e., p_a) is larger, the throughput improves when $\Phi_{1/2}$ is lower, since capture limitation goes in favor of reducing the number of decoded packets and achieving optimal number of successfully decoded ones. Overall, for different values of $\Phi_{1/2}$, the maximal throughput depends on the values of p_a and the parameter M .

Regarding the impact of the radius R on the overall throughput, similar conclusions can be drawn from Fig. 5. The radius R determines the size of the area where OWC IoT devices are located, which reflects in the distances between the devices and the OWC AP, and consequently on the received power at the AP. For example, when R is smaller, users will be close to the AP thus received packets will be decoded due to enough power to satisfy capture condition. Maximal throughput also exists for optimal value of p_a , which depends on R and M .

Adaptive control of multi-rate factor M : The above throughput analysis indicates a clear trade-off between the OWC system parameters ($R, \Phi_{1/2}$), p_a , SF and M for the system performance optimization. Given that most of the parameters may be beyond control of the system designer, we note that controlling M is an elegant way for the proposed two-tier system to operate at favourable throughput.

From Fig. 3, we note that for low number of active users (e.g., $p_a < 0.05$ when $\text{SF}=7$ and $p_a < 0.1$ when $\text{SF}=11$), the throughput is maximised for $M = 1$, i.e., when the data rates of both tiers are equal. If the number of active users increases, introducing the multi-rate functionality improves the system performance. For example, for $p_a < 0.2$ and for short OWC IoT APs and BS distance ($\text{SF}=7$ and consequently $T_{\text{rf}} = 36.6 \text{ ms}$), from Fig. 3 we observe that LoRa BS should adjust multi-rate factor to $M = 3$, i.e., to adjust the OWC slot rate

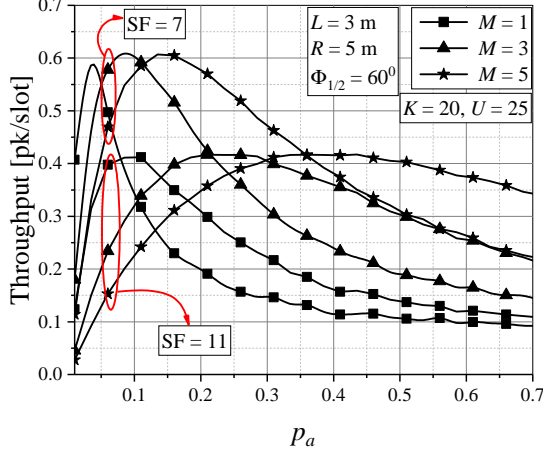


Fig. 3. Throughput vs. p_a for different M .

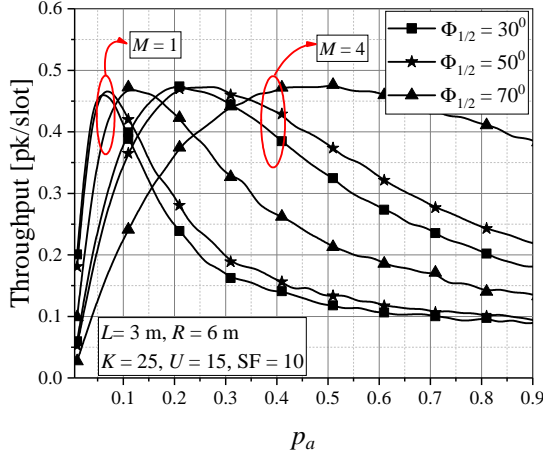


Fig. 4. Throughput vs. p_a for different values of semi-angle $\Phi_{1/2}$.

to $T_{\text{owc}} = M \cdot T_{\text{rf}} = 109.8$ ms, in order to maximise the system throughput. For a given OWC parameters, the LoRa BS could use a simple lookup table to select the value of M and consequently the OWC slot rate T_{owc} based on employed SF and estimated activity probability p_a (that can be obtained from OWC APs via user activity detection methods [19]).

Figs. 4 and 5 present the effect of adaptive control of M on the system throughput as a function of OWC system parameters. For a given OWC system parameters ($\Phi_{1/2}$, R), the LoRa BS will select the value of M that achieves the maximal throughput for a given p_a . This control mechanism can be implemented at LoRa BS as a simple lookup table that maps estimated p_a to the optimal value of M .

REFERENCES

[1] S. K. Sharma and X. Wang, "Toward massive machine type communications in ultra-dense cellular IoT networks: Current issues and machine learning-assisted solutions," *IEEE Commun. Surv. Tutor.*, 22(1), 2019.

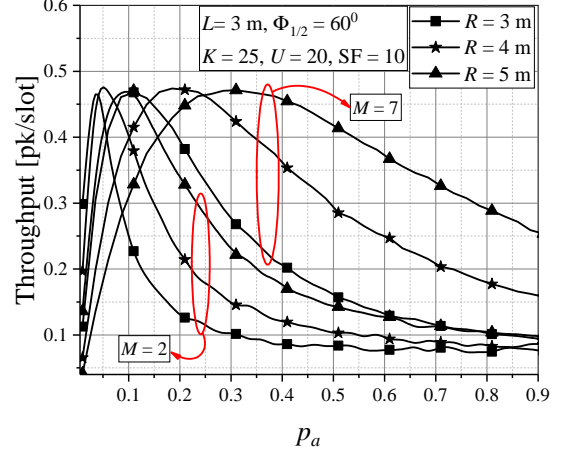


Fig. 5. Throughput vs. p_a for different values of radius R .

[2] F. Guo, F. R. Yu, H. Zhang, X. Li, H. Ji, and V. C. Leung, "Enabling massive IoT toward 6G: A comprehensive survey," *IEEE Internet Things J.*, 8(15), pp.11891-11915, 2021.

[3] A. Ikpehai, B. Adebisi, K. M. Rabie, K. Anoh, R. Ande, M. Ham-moudeh, H. Gacanin, and U. M. Mbanaso, "Low-power wide area network technologies for Internet-of-Things: A comparative review," *IEEE Internet Things J.*, 6(2), pp.2225-2240, 2018.

[4] F. Clazzer, A. Munari, G. Liva, F. Lazaro, C. Stefanovic, and P. Popovski, "From 5G to 6G: Has the time for modern random access come?" in *Proc. 1st 6G summit*, Levi, Finland, Mar. 2019.

[5] A. Laya, L. Alonso, and J. Alonso-Zarate, "Is the random access channel of LTE and LTE-A suitable for M2M communications? A survey of alternatives," *IEEE Commun. Surv. Tutor.*, 16(1), pp.4-16, 2013.

[6] L. Beltramielli, A. Mahmood, P. Österberg, and M. Gidlund, "LoRa beyond ALOHA: An investigation of alternative random access protocols," *IEEE Trans. Industr. Inform.*, 17(5), pp.3544-3554, 2020.

[7] Z. Ghassemlooy, W. Popoola, and S. Rajbhandari, *Optical Wireless Communications: System and Channel Modelling With MATLAB*. Boca Raton, FL, USA: CRC Press, 2013.

[8] L. Zhao, X. Chi, and S. Yang, "Optimal aloha-like random access with heterogeneous QoS guarantees for multi-packet reception aided visible light communications," *IEEE Trans. Wireless Commun.*, 15(11), 2016.

[9] L. Zhao, X. Chi, and W. Shi, "A QoS-driven random access algorithm for MPR-capable VLC system," *IEEE Commun. Lett.*, 20(6), 2016.

[10] T. Li, X. Chi, F. Ji, H. Shi, and S. Wang, "Optimal optical camera communication-ALOHA random access algorithm aided visible light communication system," *Opt. Eng.*, 59(7), 2020.

[11] D. Vukobratovic and F. J. Escribano, "Adaptive multi-receiver coded slotted ALOHA for indoor optical wireless communications," *IEEE Commun. Lett.*, 24(6), pp. 1308-1312, June 2020.

[12] M. Petkovic, T. Devaja, D. Vukobratovic, F. J. Escribano, and C. Stefanovic, "Reliability analysis of slotted aloha with capture for an OWC-based IoT system," in *Proc. ISWCS 2021*, Berlin, Germany, 2021.

[13] T. Devaja, M. Petkovic, A. Munari, F. Clazzer, M. Beko, and D. Vukobratovic "Massive Machine-Type Communications via Hybrid OWC/RF Networks," in *Proc. CSNDSP 2022*, Porto, Portugal, 2022.

[14] M. Petkovic, D. Vukobratovic, A. Munari, and F. Clazzer, "Relay-aided slotted aloha for optical wireless communications," in *Proc. CSNDSP 2020*, Porto, Portugal, 2020.

[15] D. Zheng, Y. D. Yao, C. Graff, and T. Cook, "Two-tier slotted aloha in mobile ad hoc networks," in *Proc. IEEE MILCOM 2007*, 2007.

[16] O. Georgiou, U. Raza, "Low power wide area network analysis: Can LoRa scale?," *IEEE Wireless Commun. Lett.*, 6(2), 2017.

[17] C. Goursaud, J.-M. Gorce, "Dedicated networks for IoT: PHY/MAC state of the art and challenges," *EAI endorsed TloT*, 2015.

[18] K. K. Wong, T. O'Farrell, "Spread spectrum techniques for indoor wireless IR communications," *IEEE Wireless Commun.*, 10(2), 2003.

[19] V. Boljanović, D. Vukobratović, P. Popovski, C. Stefanović, "User activity detection in massive random access: Compressed sensing vs. coded slotted ALOHA," *IEEE SPAWC 2017*, Kyoto, Japan, 2017.